

# **Influence of the composition of $M_{78}Si_9B_{13}$ metallic glasses on their structural stability**

EWA JAKUBCZYK<sup>1</sup>, ZDZISŁAW STĘPIEŃ<sup>1</sup>, MIECZYŚŁAW JAKUBCZYK<sup>2</sup>

<sup>1</sup>Institute of Physics, Jan Długosz University, al. Armii Krajowej 13/15, 42-201 Częstochowa, Poland

<sup>2</sup>Institute of Chemistry and Environmental Protection, Jan Długosz University, al. Armii Krajowej 13/15, 42-201 Częstochowa, Poland

The structural stability of  $Co_{78}Si_9B_{13}$  and  $Fe_{78}Si_9B_{13}$  metallic glasses was investigated by differential scanning calorimetry (DSC), X-ray diffraction, Hall effect and electrical resistivity methods. It was found that at first isochronal annealing leads to the formation of  $\alpha$ -M (M = Co, Fe) phases. This process is followed by the formation of  $M_2B$  phases. The phases were identified by X-ray diffraction method and their structures were confirmed with the use of quantum chemistry method. The creation of crystalline phases decreases abruptly the Hall and electrical resistivities. The alloy containing Fe appeared to have a much wider range of structural stability.

Keywords: metallic glasses, crystallization, Hall effect.

## **1. Introduction**

A rapid solidification from the liquid state leads to the formation of a metastable amorphous structure. Depending on the method of such a rapid solidification as well as the composition of the alloy, the obtained metastable structures are characterized by supersaturation in defects, an extension of solid solubility above the equilibrium limit, formation of metastable crystalline, quasicrystalline or glassy phases [1]. Metallic glasses are obtained just through the rapid solidification, so they exhibit short range ordering (SRO). The metastability is understandable because atoms during a quick transition from liquid to solid state do not take up the equilibrium position, in which they would have lower energy. As a consequence, the structural relaxations take place, which leads, through the changes of the chemical and topological short range ordering (CSRO and TSRO) as well as in medium range ordering (MRO), to a polycrystalline state [2, 3]. The initiation and the kinetics of the crystallization process depend on many factors. It is known that defects in the solidified alloys can act as nucleation sites or can accelerate crystal growth. The differences in the density of

defects may influence kinetics of precipitation or decomposition of metastable phases. Therefore, due to their anisotropic microstructure, fluctuations of the density of defects in metallic glass ribbons shall lead to a complicated transformation to a crystalline state. Phase transitions in the crystallization process of metallic glasses have different kinetics depending on the various possible types of transformation. Depending on the alloy composition, transformation can occur due to the following typical reactions: polymorphous, eutectoid, primary and peritectoid crystallization [1]. Research concerning phase transitions in metallic glasses is intensive both from scientific point of view and for application of these materials. In our laboratory we have investigated the structural and physical properties of  $\text{Fe}_{78-x}\text{Co}_x\text{Si}_9\text{B}_{13}$  metallic glasses. In this paper, we concentrate on the analysis of the influence of composition on the structure relaxation caused by isochronal annealing. For the reason of comparison we have chosen the most distinctive glasses from the family, *i.e.*,  $\text{Fe}_{78}\text{Si}_9\text{B}_{13}$  and  $\text{Co}_{78}\text{Si}_9\text{B}_{13}$ . The thermal stimulation of the structural changes, which finally can lead to the phase transitions is realized by isochronal or isothermal annealing. Naturally, the structural changes coincide with the changes of physical properties, and the latter ones are especially significant when a phase transition occurs. The standard methods applied to investigation of phase transitions are: differential scanning calorimetry (DSC), X-ray diffraction, electrical resistivity and optical or electron microscopy. The aim of this paper is to study phase transitions also through investigation of the Hall effect in metallic glasses  $\text{M}_{78}\text{Si}_9\text{B}_{13}$  ( $\text{M} = \text{Fe}, \text{Co}$ ), which were isochronally annealed (4 h) at different temperatures ranging from 573 to 823 K.

## 2. Experimental

The ribbons of metallic glasses  $\text{Fe}_{78}\text{Si}_9\text{B}_{13}$  and  $\text{Co}_{78}\text{Si}_9\text{B}_{13}$  were prepared by the roller quenching method. DSC measurements were carried out using an STA-409 NETZSCH apparatus under an argon stream at a constant heating rate of 5 K/min. Measurements of the electrical and Hall resistivities and X-ray diffraction were done at room temperature for the as-received as well as isochronally (4 h) annealed samples at different temperatures (573–823 K) in inert argon atmosphere. The X-ray studies were performed using DRON-2.0 diffractometer with  $\text{Mo } K_\alpha$  radiation. The Hall voltage was measured by a constant current method at constant magnetic field [4]. The electrical resistivity was also measured in the d.c. regime. The quantum chemical calculations of the total energy of the created phases were done using a semi-empirical method of HyperChem 6.0 program.

## 3. Results and discussion

The result of the investigation of non-isothermal crystallization process carried out for  $\text{Fe}_{78}\text{Si}_9\text{B}_{13}$  and  $\text{Co}_{78}\text{Si}_9\text{B}_{13}$  metallic glasses by DSC at a constant heating rate of 5 K/min shows that devitrification of both alloys consists of two main stages. In the case of  $\text{Co}_{78}\text{Si}_9\text{B}_{13}$  the exotherm peaks in DSC curve are widely separated, while those

Table. Temperature of the peaks of the first  $T_1$  and second  $T_2$  stages of crystallization.

	$Co_{78}Si_9B_{13}$	$Fe_{78}Si_9B_{13}$
$T_1$ [K]	705.5	783.1
$T_2$ [K]	833.8	810.5

of  $Fe_{78}Si_9B_{13}$  are closely situated. The peaks responsible for the first stage of crystallization are wide and the others are sharp. Positions of the maximum of the peaks referring to the first and second stage of crystallization are listed in the Table.

Stimulation of the structural changes was initiated by annealing at 573 K, which is much less than the temperature of the first stage of crystallization for both  $Co_{78}Si_9B_{13}$  and  $Fe_{78}Si_9B_{13}$ .

In order to analyse the structural changes and identify the phases formed out of the matrix an X-ray investigation for the as-received as well as annealed samples was performed. Diffraction patterns for both alloys are presented in Fig. 1. As one can see the crystallization of the metallic glasses begins after the annealing at 648 and 723 K for alloys containing Co and Fe, respectively. A qualitative analysis of the phases formed proves that these are the phases of the transition metals, i.e.,  $\alpha$ -Co and  $\alpha$ -Fe [6, 7]. The amorphous matrix is enriched with boron after the crystalline phase of metal

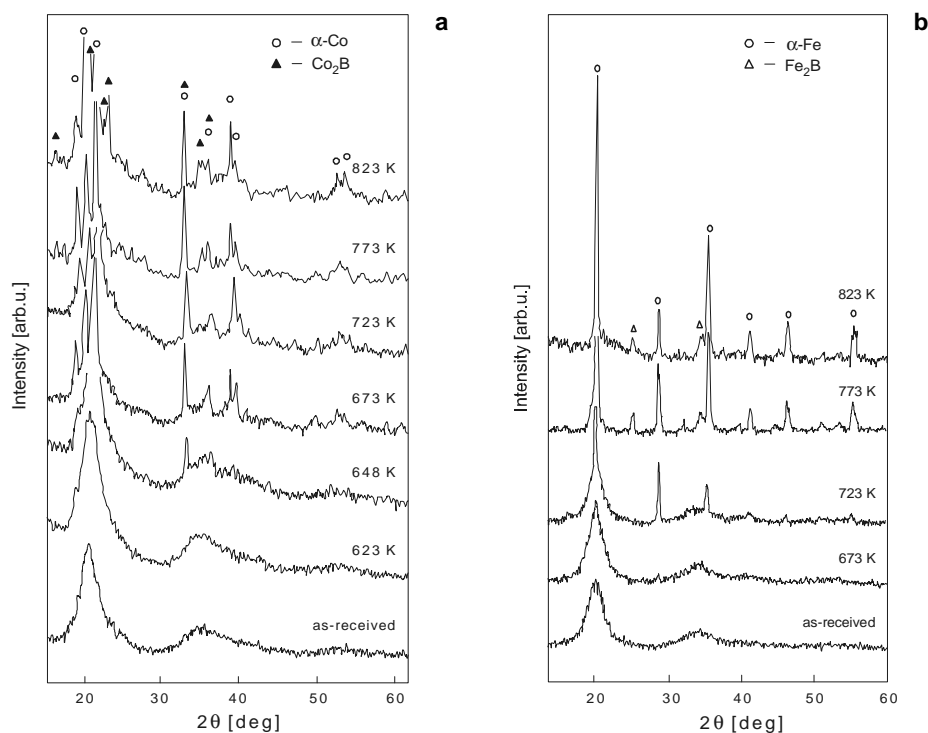


Fig. 1. X-ray diffraction patterns for samples of alloys:  $Co_{78}Si_9B_{13}$  (a) and  $Fe_{78}Si_9B_{13}$  (b).

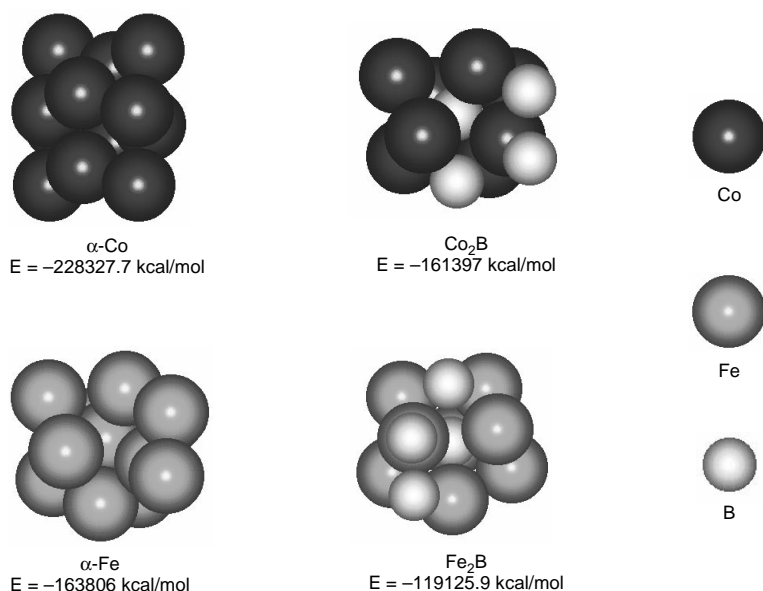


Fig. 2. Clusters of the formed phases.

is created, and this leads to crystallization of  $\text{Co}_2\text{B}$  and  $\text{Fe}_2\text{B}$  phases, formed after annealing at 773 K.

To verify the sequence of the phases determined on the basis of X-ray diffraction, quantum chemistry calculations of the total energy of the model clusters representing the alloys under investigation (Fig. 2) were carried out by semi-empirical method (ZINDO/1). Values of the total energy of  $\alpha\text{-Co}$  clusters are smaller than those of  $\text{Co}_2\text{B}$  clusters and the energies obtained for  $\alpha\text{-Fe}$  and  $\text{Fe}_2\text{B}$  are in analogous relation. These results prove that in both alloys at first the metal phases crystallize out of amorphous matrix during the annealing because they require lower energy and only after annealing at higher temperatures the borides crystallize. The differences between the calculated values of the energy of metal and boride phases are 66930.7 kcal/mol and 44680.1 kcal/mol for  $\text{Co}_{78}\text{Si}_9\text{B}_{13}$  and  $\text{Fe}_{78}\text{Si}_9\text{B}_{13}$ , respectively. This proves that the difference between the temperature of crystallization of metal and boride phases in the alloy with Co is greater than that of the alloy with Fe.

The electrical resistivity belongs to a family of the properties of electronic transport and its measurement is a standard method of defining structural transformations [5]. Now, we will consider the influence of magnetic field on the transport properties in ferromagnetic amorphous materials during transformation. Figures 3 and 4 show the results of investigation of the Hall resistivity  $\rho_H$  as a function of external magnetic field  $B_0$  for samples in as-received state and samples annealed isochronally at different temperatures. With an increase of the annealing temperature the  $\rho_H$  decreases. For the  $\text{Co}_{78}\text{Si}_9\text{B}_{13}$  alloy the first lowering of the curves  $\rho_H = f(B_0)$  occurs after annealing

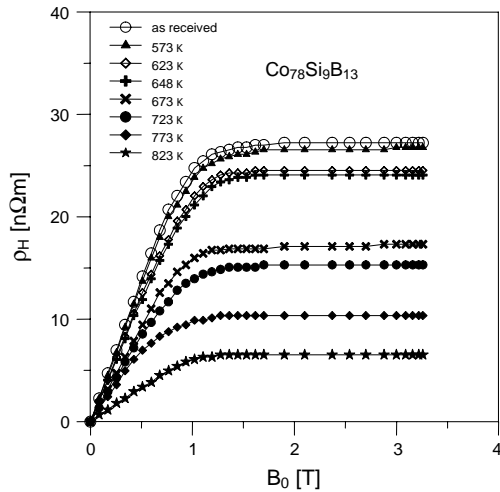


Fig. 3. Hall resistivity  $\rho_H$  as a function of the applied magnetic induction  $B_0$  for samples of  $Co_{78}Si_9B_{13}$  alloy annealed at different temperatures.

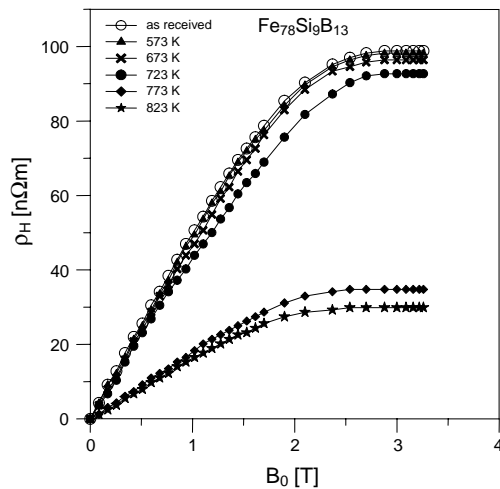


Fig. 4. Hall resistivity  $\rho_H$  as a function of the applied magnetic induction  $B_0$  for samples of  $Fe_{78}Si_9B_{13}$  alloy annealed at different temperatures.

at 623 K and the next distinct lowerings of the curves are observed after annealing at 673 and 773 K. For the  $Fe_{78}Si_9B_{13}$  alloy the abruptly decline of curves  $\rho_H = f(B_0)$  occurs after annealing at 723 and 773 K. On the basis of the X-ray diffraction investigations we can state that as a result of annealing of  $Co_{78}Si_9B_{13}$  alloy at 648 and 773 K and the  $Fe_{78}Si_9B_{13}$  alloy at 723 and 773 K creation of crystalline phases begins (Fig. 1). The diffraction patterns (Fig. 1a) as well as the result of investigation of

the Hall resistivity (Fig. 3) prove that the alloy with Co is characterized by a more complicated transformation process. The annealing at temperatures  $623 \text{ K} < T < 773 \text{ K}$  leads to the formation of stable  $\text{Co}_2\text{B}$  phase through the metastable medium states.

The ordinary Hall effect comes from the Lorentz force acting on the charge carriers in nonmagnetic materials. The most common geometry for the measurement of the Hall effect is the measurement of transverse electric field  $\mathbf{E}_H(0, E_H, 0)$ , appearing across a sample, when magnetic induction  $\mathbf{B}_0(0, 0, B_0)$  and the current density  $\mathbf{J}(J_x, 0, 0)$  are applied:

$$\mathbf{E}_H = R_H(\mathbf{J} \times \mathbf{B}_0). \quad (1)$$

The Hall effect is often described by the Hall resistivity  $\rho_H$ :

$$\rho_H = E_H/J_x = R_H B_0 \quad (2)$$

where  $R_H$  is the Hall coefficient. In the ferromagnetic materials the Hall resistivity must be written as [8–12]:

$$\rho_H = R_0 B_0 + \mu_0 R_S M \quad (3)$$

where the first term is the ordinary Hall resistivity ( $\rho_{H0} \propto B_0$ ) and the second term is the spontaneous Hall effect ( $\rho_{HS} \propto M$ ). All the curves from Figs. 3 and 4 are described by Eq. (3). The  $\rho_{HS}$  represents the initial part of the curves and  $\rho_{H0}$  part of the curves for  $B_0 > \mu_0 M_S$ , *i.e.*, above the magnetisation saturation. The  $\rho_{HS}$  is connected with a ferromagnetic state of a sample and determined by the following mechanisms: a spin-orbit interaction, a skew scattering and a side jump [10, 11]. These mechanisms decrease the mean free path of carriers. Figure 5 shows, for both alloys, the relative changes of the electrical resistivity (related to the resistivity of the as-received state) versus the annealing temperature. The  $\text{Fe}_{78}\text{Si}_9\text{B}_{13}$  alloy shows an increase of  $\Delta\rho/\rho_0$  value in the initial range of annealing, which is connected with the structural changes

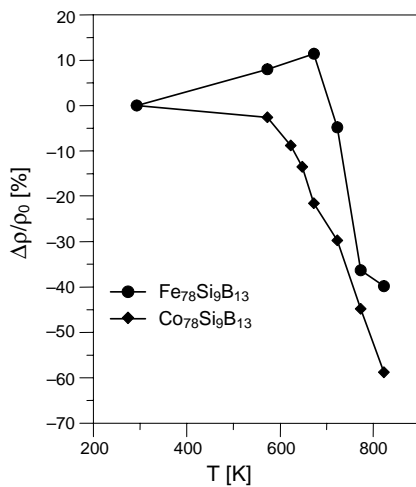


Fig. 5. Relative electrical resistivity  $\Delta\rho/\rho_0$  as a function of annealing temperature  $T$  for samples of  $\text{Co}_{78}\text{Si}_9\text{B}_{13}$  and  $\text{Fe}_{78}\text{Si}_9\text{B}_{13}$  alloys.

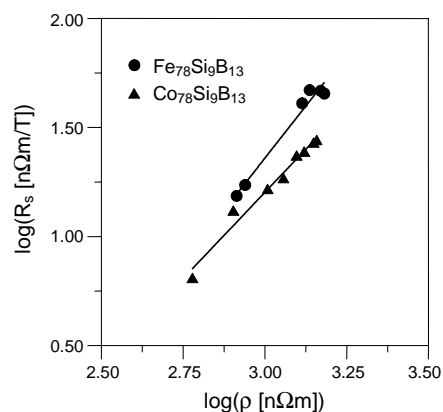


Fig. 6. Dependence  $\log(R_s)$  vs.  $\log(\rho)$  for  $Co_{78}Si_9B_{13}$  and  $Fe_{78}Si_9B_{13}$  alloys annealed at different temperatures.

of TSRO type. A decrease of electrical resistivity during the crystallization is caused by an increase of the free path of carriers in ordered structure in medium and long range.

According to Berger and Bergmann the spontaneous Hall coefficient  $R_s$  is described by the dependence [10–12]:

$$R_s = a\rho + b\rho^2 \quad (4)$$

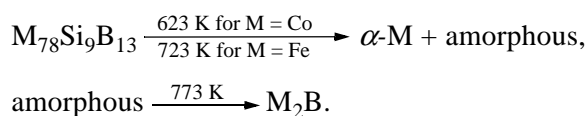
where  $a$  and  $b$  are constants roughly independent of temperature and  $\rho$  is the resistivity. The first term of Eq. (4) is responsible for the classical asymmetric scattering of charge carriers and the second term describes the quantum effect and corresponds to the lateral displacement of the charge carrier trajectory at the point of scattering, *i.e.*, the side jump.

The dependence of  $\log(R_s)$  on  $\log(\rho)$  gives the exponent  $n$  in relation  $R_s \propto \rho^n$  and by such means it can be concluded which type of scattering is dominant for the spontaneous Hall effect. Figure 6 represents these dependences for both alloys. The calculated exponents  $n$  for  $Co_{78}Si_9B_{13}$  and  $Fe_{78}Si_9B_{13}$  are, respectively, 1.58 and 1.91. The values  $n$  indicate that during the crystallization process the side jump is the dominant scattering. The structural changes appear in the measurements of the electrical and Hall resistivities after annealing at temperatures lower than in X-ray diffraction studies and DSC. This demonstrates that the methods involving the electronic transport are more sensitive to the structural changes.

#### 4. Conclusions

Substituting Co with Fe in alloys  $M_{78}Si_9B_{13}$  ( $M = Co, Fe$ ) widens the range of the structural stability. The investigation of the Hall effect proves that the  $Co_{78}Si_9B_{13}$  and  $Fe_{78}Si_9B_{13}$  alloys start to crystallize after annealing at 623 and 723 K, respectively.

Both alloys show two stages of crystallization which can be described by the following scheme:



The first stage of crystallization of both alloys occurs as a result of the primary crystallization and the second stage as a result of the polymorphous crystallization.

The substitution of Co with Fe drastically increases the Hall resistivity in the as-received state.

The Hall and electrical resistivities decrease abruptly after the crystallization of the phase during the transformation to polycrystalline state.

During the crystallization process the ferromagnetic order is conserved. The dominant scatterings of charge carriers are the side jump.

## References

- [1] KÖSTER U., *Phase transformations in rapidly solidified alloys*, Key Engineering Materials **81-83**, 1993, pp. 647–62.
- [2] VAN DEN BEUKEL A., RADELAAR S., *On the kinetics of structural relaxation in metallic glasses*, Acta Metallurgica **31**(3), 1983, pp. 419–27.
- [3] VAN DEN BEUKEL A., *On the kinetics of structural relaxation in metallic glasses*, Key Engineering Materials **81-83**, 1993, pp. 3–16.
- [4] JAKUBCZYK E., *Structural phase transition of Co-Ni-Si-B amorphous alloy*, Acta Physica Polonica A **99**(6), 2001, pp. 673–81.
- [5] KOMATSU T., SATO S., MATUSIDA K., *Compositional dependence of resistivity changes during structural relaxation in (Co, Fe)<sub>75</sub>Si<sub>10</sub>B<sub>15</sub> metallic glasses*, Acta Metallurgica **34**(10), 1986, pp. 1899–904.
- [6] KUZMA YU.B., CHABAN N.F., *Dwojnyje i trojnyje sistemi sodierzaszczije bor*, Metallurgija, Moskwa, 1990.
- [7] VILLARS P., *Pearson's Handbook Desk Edition, Crystallographic Data for Intermetallic Phases*, ASM International, Materials Park, USA 1997.
- [8] HURD C.M., *The Hall Effect in Metals and Alloys*, Plenum Press, New York, London 1972, p. 153.
- [9] HEINEMANN K., BARNER K., *Transport and magnetic properties of amorphous (Fe<sub>1-x</sub>Mn<sub>x</sub>)<sub>75</sub>P<sub>15</sub>C<sub>10</sub> alloys*, Journal of Magnetism and Magnetic Materials **42**(3), 1984, pp. 291–4.
- [10] BERGER L., BERGMANN G.N., [In] *The Hall Effect and Its Applications*, [Eds.] Chien C.L., Westgate C.R., Plenum Press, New York 1980, p. 55.
- [11] MCGUIRE T.R., GAMBINO R.J., O'HANDLEY R.C., [In] *The Hall Effect and Its Applications*, [Eds.] Chien C.L., Westgate C.R., Plenum Press, New York 1980, p. 137.
- [12] STOBIECKI T., PRZYBYLSKI M., *Spontaneous Hall effect and magnetization of Fe-(B,Zr) and Co-Mo amorphous films*, Physica Status Solidi B **134**(1), 1986, pp. 131–9.

*Received June 6, 2005  
in revised form August 20, 2005*